EURASIP Journal on Wireless Communications and Networking 2004:2, 309–321

Iterative MIMO Turbo Multiuser Detection and Equalization for STTrC-Coded Systems with Unknown Interference

Nenad Veselinovic
Centre for Wireless Communications, University of Oulu, Tutkijantie 2E, P.O. Box 4500, 90014 Oulu, Finland
Email: nenad.veselinovic@ee.oulu.fi

Tad Matsumoto
Centre for Wireless Communications, University of Oulu, Tutkijantie 2E, P.O. Box 4500, 90014 Oulu, Finland
Email: tadashi.matsumoto@ee.oulu.fi

Markku Juntti
Centre for Wireless Communications, University of Oulu, Tutkijantie 2E, P.O. Box 4500, 90014 Oulu, Finland
Email: markku.juntti@ee.oulu.fi

Received 30 November 2003; Revised 16 April 2004

Iterative multiuser detection in a single-carrier broadband multiple-input multiple-output (MIMO) system is studied in this paper. A minimum mean squared error (MMSE) low-complexity multiuser receiver is derived for space-division multiple-access (SDMA) space-time trellis-coded (STTrC) systems in frequency-selective fading channels. The receiver uses MMSE filtering to jointly detect several transmit antennas of the user of interest, while the interference from the undetected transmit antennas, cochannel interference (CCI), and intersymbol interference (ISI) are all cancelled by the soft cancellation. The performances of two extreme receiver cases are evaluated. In the first case, only one transmit antenna of the user of interest is detected at a time and the remaining ones are cancelled by soft cancellation. In the second case, all the transmit antennas are detected jointly. The comparison of the two cases shows improvement with the latter one, both in single-user and multiuser communications and in the presence of unknown cochannel interference (UCCI). It is further shown that in the multiuser case, the proposed receivers approach the corresponding single-user bounds. The number of receive antenna elements required to achieve single-user bound is thereby equal to the number of users and not to the total number of transmit antennas.

Keywords and phrases: turbo equalization, multiuser detection, space-time codes, cochannel interference.

1. INTRODUCTION

The scarcity of the frequency spectrum resources and the ever-growing demand for new broadband services imposes a need for the bandwidth-efficient transceiver schemes. Signal transmission and reception using multiple-transmit and multiple-receive antennas over a multiple-input multiple-output (MIMO) channel is one of the most promising approaches for increasing the link capacity and the achievable data rates [1]. Two key approaches have been developed to make effective use of the benefits of the MIMO channels. The first one is the Bell-Labs-layered-space-time architecture (BLAST) [2], where independent signals are transmitted from different transmit antennas. Another technique that combines the benefits of transmit diversity and channel coding in an efficient manner is space-time coding either in a form of space-time block coding (STBC) [3] or space-time trellis coding (STTrC) [4]. This paper focuses on STTrC-coded systems.

STTrC codes have originally been developed for frequency flat-fading channels. In order to meet the requirements for high-data-rate transmission, their extension to frequency-selective channels and performance in such scenarios are of great interest. The performance of STTrC codes in unequalized frequency-selective channels was studied in [5, 6], where it was shown that the dominant factor on their performance is the intersymbol interference (ISI), that causes inevitable error floor in large signal-to-noise ratio (SNR) range. To solve this problem, two research directions have been followed in recent years. One of them is a combination of orthogonal-frequency-division-multiplexing (OFDM) and decoding [7], which allows one

to perform signal processing for a set of frequency flat-fading channels. The other approach is a combination of equalization and decoding for single-carrier communications. The optimal receiver for the frequency-selective channels is the *maximum a posteriori* (MAP) equalizer usually implemented by means of the BCJR algorithm [8]. Its complexity, however, grows exponentially with the number of multipath components. Moreover, in the channel-coded systems, the optimal receiver is the one that performs joint equalization and decoding and its complexity is exponential in the product of the number of multipath components and the code memory length. Therefore, it is impractical in broadband systems, and low complexity schemes are of a particular interest. The problem of complexity of the optimal joint equalization and decoding can be effectively solved by iterative (turbo) equalization principle that was introduced in [9]. Further complexity reductions have been mainly based on simplifications of the equalization part. This paper focuses on the low-complexity turbo equalization for single-carrier communications using STTrC codes.

Joint iterative equalization and decoding of STTrC codes is introduced in [10], where the optimal MAP equalizer is used. Its low-complexity extension is proposed in [11], where channel shortening takes place first, and the reduced complexity MAP algorithm is performed afterwards. The technique results in relatively low-performance degradation when compared to the optimal receiver. In the case of decision feedback equalization (DFE) combined with STTrC-decoder in an iterative manner, a method for complexity reduction was studied by [12, 13]. This method is based on the decoupling between the real and imaginary parts of the received signal, resulting in a reduced total number of equalizer states. An equalizer based on soft interference cancellation and MMSE filtering was proposed in [14] for a convolutionally coded system with diversity signal reception. The receiver can be seen as an extension of the idea introduced for code-division multiple-access (CDMA) in [15]. It was further extended to cover higher-order modulations in [16, 17], where further complexity reduction methods were proposed as well. In [18], the idea was applied to the multiuser diversity signal detection with convolutional codes. The reduced complexity version of the receiver, based on matched filter approximation, was proposed in [19]. An STTrC coded multiuser system in frequency flat MIMO channels was considered in [20]. It employs iterative multiuser detection schemes similar to those of [15, 18].

In some situations, the unknown cochannel interference (UCCI) can be present in the channel apart from the users that are to be detected. Those users can originate from the undetected users in the same cell, from the other-cell interference, or from other communication systems. In [21], an iterative UCCI suppression method has been studied, which is based on the covariance-matrix-estimation technique. Subspace estimation methods for the UCCI suppression were considered in [20, 22] in CDMA and SDMA systems, respectively. A noniterative receiver for detection of STTrC codes in the presence of UCCI was introduced in [23] in frequency-flat-fading channels. The method of [23] is based on joint detection of all the transmit antennas' signals using MMSE receiver presented in [24]. A similar solution was proposed in [25] for the orthogonal transmission using STBC codes in flat-fading channels. In [23, 25], however, the MMSE filters are different so that the outputs of the latter one are the combined signals from all the receive antennas, while the outputs of the former are the separated outputs for each receive antenna.

In this paper, new low-complexity turbo equalization schemes for the multiuser MIMO-STTrC-coded system are derived. The first part of the studied receivers is soft cancellation of both ISI and cochannel interference (CCI). The second part is a linear MMSE filtering that is used to cope with the residual interference after soft cancellation and UCCI if the latter is present. The degrees-of-freedom (DoF) of the MMSE receiver are thereby decreased depending on the significance of the residual interference and UCCI. The receiver can be seen as a combination of those considered in [20, 25], and their extension to frequency-selective channels. Assuming that each transmitter has N_T transmit antennas, the receiver is derived for the general case of jointly detecting signals in the N_T/n_0 sets containing n_0 transmit antennas of one particular user, where N_T is an integer multiple of n_0. The derived receiver's performance in special cases corresponding to $n_0 = 1$ and $n_0 = N_T$ is studied through simulations. The case $n_0 = 1$ can be seen as an extension of the receiver proposed in [20] to the frequency selective channels. The cases of $1 \leq n_0 \leq N_T$ are a further receiver extensions where several transmit antennas are detected jointly. The aim of joint detection of several transmit antennas' signals is to preserve the DoFs of the receiver. In case of $n_0 = N_T, N_T - 1$, the DoFs are preserved.

The UCCI mitigation capability of the proposed receiver is attained by using the iterative covariance estimation technique shown in [21]. It should be noted that the receiver proposed in [20] requires the knowledge of the UCCI channel matrix. Unlike [20], the method of [21] requires only a covariance matrix estimate of the UCCI-plus-noise and it is therefore less complex.

The rest of the paper is organized as follows. Section 2 describes system model. Section 3 presents the proposed receiver and its special cases for which either one antenna or all antennas are detected simultaneously. Section 4 describes the maximum-likelihood (ML) receiver with perfect feedback, whose performance curve is used as a lower bound on the proposed receivers' performance. Section 5 presents numerical results. The paper is concluded in Section 6.

Notation. In the sequel, the following notations were adopted.

(i) $\widehat{(\cdot)}$ denotes the estimate of $(\cdot)$.

(ii) $(\cdot)_k$, $(\cdot)^{(n)}$, and $(\cdot)(i)$ denote dependence of $(\cdot)$ on the kth user, nth transmit antenna, and timing index i, respectively.

(iii) $\overline{(\cdot)}$ and $\widetilde{(\cdot)}$ denote the variable obtained by replacing the corresponding entries of $(\cdot)$ using soft *a posteriori* and *extrinsic* feedback, respectively.

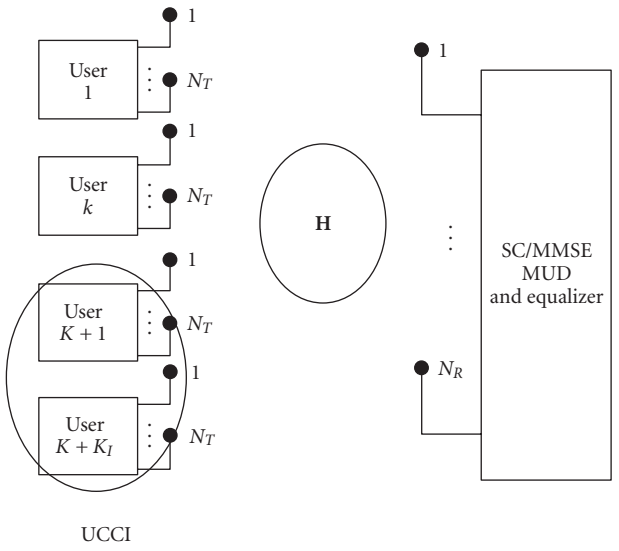

Figure 1: System model.

(iv) $(\cdot)^{\langle \gamma \rangle}$ denotes the dependence of $(\cdot)$ on the γth antenna set, where $\gamma = 1, \ldots, N_T/n_0$.

(v) $(\cdot)^{\mathrm{T}}$, $(\cdot)^{H}$, and $\mathrm{E}\{(\cdot)\}$ denote transpose, conjugate transpose, and expectation of $(\cdot)$, respectively.

(vi) $[(\cdot)]_{m,n}$, $[(\cdot)]_m$ denote the (m,n)th element of $(\cdot)$ if $(\cdot)$ is a matrix and the mth element of $(\cdot)$ if $(\cdot)$ is a vector, respectively.

2. SYSTEM AND RECEIVED SIGNAL MODEL

Figures 1 and 2 describe the system model and the kth user's transmitter block diagram assumed in this paper, respectively. Each of $K + K_I$ users encodes bit information sequence $c_k(i)$, $k = 1, \ldots, K + K_I$, $i = 1, \ldots, Bk_0$, using a rate k_0/N_T STTrC code, where N_T and B are the numbers of transmit antennas and frame length in symbols, respectively. The users indexed by $k = 1, \ldots, K$ are the users of interest to be detected and the others indexed by $k = K + 1, \ldots, K_I$ are unknown users. The encoded sequences $b_k(i) \in \mathbb{Q}$, $i = 1, \ldots, BN_T$, are first grouped in B blocks of N_T symbols, where $\mathbb{Q} = \{\alpha_1, \ldots, \alpha_{2^{k_0}}\}$ denotes the modulation alphabet of M-phase-shift-keying (M-PSK). However, it is straightforward to extend the receiver derivations to quadrature-amplitude-modulation (QAM) schemes. The coded sequence is then interleaved so that the positions within blocks of length N_T remain unchanged, but the positions of the blocks themselves are permuted within a frame according to the user-specific interleaver pattern. Thereby the rank properties of the STTrC codes are preserved [26]. The interleaved sequences are then headed by user-specific training sequences consisting of TN_T symbols. The entire frame is serial-to-parallel converted, resulting in the sequences $b_k^{(n)}(i)$, $n = 1, \ldots, N_T$, $i = 1, \ldots, B + T$, and transmitted with N_T transmit antennas through the frequency-selective channel.

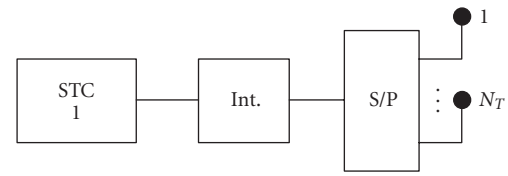

Figure 2: Transmitter block diagram for the first user.

After coherent demodulation in the receiver, the signals from each of N_R receive antennas are sampled in time domain to capture the multipath components. Observing the signals from different transmit antennas of different users as the virtual users and arranging them in the vector form similarly as in [18, 20], we form the space-time representation of the received signal at time instant i given by

$$\mathbf{y}(i) = \underbrace{\mathbf{H}\mathbf{u}(i)}_{\text{desired}} + \underbrace{\mathbf{H}_I\mathbf{u}_I(i)}_{\text{UCCI}} + \underbrace{\mathbf{n}(i)}_{\text{noise}}, \quad i = 1, \ldots, T + B, \tag{1}$$

where $\mathbf{y}(i) \in \mathbb{C}^{LN_R \times 1}$ is space-time sampled received signal vector, given by

$$\mathbf{y}(i) = \left[\mathbf{r}^{\mathrm{T}}(i + L - 1), \ldots, \mathbf{r}^{\mathrm{T}}(i)\right]^{\mathrm{T}}, \tag{2}$$

where

$$\mathbf{r}(i) = \left[r_1(i), \ldots, r_{N_R(i)}\right]^{\mathrm{T}} \in \mathbb{C}^{N_R \times 1}, \tag{3}$$

L is the number of paths of the frequency-selective channel, and $r_m(i)$ denotes the signal sample obtained after matched filtering at the mth receive antenna. Channel matrix $\mathbf{H}$ has the form of

$$\mathbf{H} = \begin{bmatrix} \mathbf{H}(0) & \cdots & \mathbf{H}(L-1) & \cdots & \mathbf{0} \\ \vdots & \ddots & & \ddots & \vdots \\ \mathbf{0} & \cdots & \mathbf{H}(0) & \cdots & \mathbf{H}(L-1) \end{bmatrix} \in \mathbb{C}^{LN_R \times KN_T(2L-1)},$$

$$\mathbf{H}(l) = \begin{bmatrix} h_{1,1}^{(1)}(l) & \cdots & h_{1,1}^{(N_T)}(l) & \cdots & h_{K,1}^{(1)}(l) & \cdots & h_{K,1}^{(N_T)}(l) \\ \vdots & \ddots & \vdots & \ddots & \vdots & \ddots & \vdots \\ h_{1,N_R}^{(1)}(l) & \cdots & h_{1,N_R}^{(N_T)}(l) & \cdots & h_{K,N_R}^{(1)}(l) & \cdots & h_{K,N_R}^{(N_T)}(l) \end{bmatrix} \in \mathbb{C}^{N_R \times KN_T}, \tag{4}$$

where $h_{k,m}^{(n)}(l)$ denotes the lth path complex gain between kth user's nth transmit antenna and mth receive antenna. Similarly, $\mathbf{H}_I$ is defined as

$$\mathbf{H}_I = \begin{bmatrix} \mathbf{H}_I(0) & \cdots & \mathbf{H}_I(L-1) & \cdots & \mathbf{0} \\ \vdots & \ddots & & \ddots & \vdots \\ \mathbf{0} & \cdots & \mathbf{H}_I(0) & \cdots & \mathbf{H}_I(L-1) \end{bmatrix} \in \mathbb{C}^{LN_R \times K_I N_T(2L-1)} \tag{5}$$

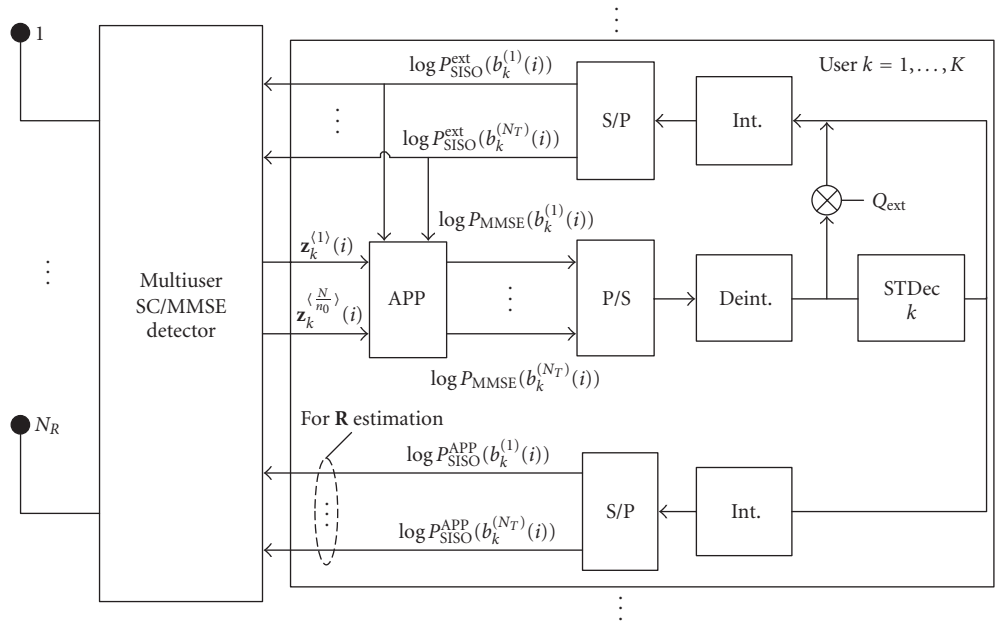

Figure 3: Iterative receiver block diagram.

with

$$\mathbf{H}_I(l) = \begin{bmatrix} h^{(1)}_{K+1,1}(l) & \cdots & h^{(N_T)}_{K+1,1}(l) & \cdots & h^{(1)}_{K+K_I,1}(l) & \cdots & h^{(N_T)}_{K+K_I,1}(l) \\ \vdots & \ddots & \vdots & \ddots & \vdots & \ddots & \vdots \\ h^{(1)}_{K+1,N_R}(l) & \cdots & h^{(N_T)}_{K+1,N_R}(l) & \cdots & h^{(1)}_{K+K_I,N_R}(l) & \cdots & h^{(N_T)}_{K+K_I,N_R}(l) \end{bmatrix} \in \mathbb{C}^{N_R \times K_I N_T}. \tag{6}$$

The vectors $\mathbf{u}(i)$ and $\mathbf{u}_I(i)$ denote the desired and unknown users' sequences, respectively, which are defined as

$$\begin{aligned} \mathbf{u}(i) &= \left[\mathbf{b}^{\mathrm{T}}(i+L-1), \ldots, \mathbf{b}^{\mathrm{T}}(i), \ldots, \mathbf{b}^{\mathrm{T}}(i-L+1)\right]^{\mathrm{T}} \\ &\in \mathbb{Q}^{KN_T(2L-1)\times 1}, \\ \mathbf{u}_I(i) &= \left[\mathbf{b}_I^{\mathrm{T}}(i+L-1), \ldots, \mathbf{b}_I^{\mathrm{T}}(i), \ldots, \mathbf{b}_I^{\mathrm{T}}(i-L+1)\right]^{\mathrm{T}} \\ &\in \mathbb{Q}^{K_I N_T(2L-1)\times 1} \end{aligned} \tag{7}$$

with

$$\begin{aligned} \mathbf{b}(i) &= \left[b_1^{(1)}(i), \ldots, b_1^{(N_T)}(i), \ldots, b_K^{(1)}(i), \ldots, b_K^{(N_T)}(i)\right]^{\mathrm{T}} \\ &\in \mathbb{Q}^{KN_T\times 1}, \\ \mathbf{b}_I(i) &= \left[b_{K+1}^{(1)}(i), \ldots, b_{K+1}^{(N_T)}(i), \ldots, b_{K+K_I}^{(1)}(i), \ldots, b_{K+K_I}^{(N_T)}(i)\right]^{\mathrm{T}} \\ &\in \mathbb{Q}^{K_I N_T\times 1}. \end{aligned} \tag{8}$$

Vector $\mathbf{n}(i) \in \mathbb{C}^{LN_R\times 1}$ contains the spatially and temporally white additive Gaussian noise (AWGN) samples with covariance $\mathrm{E}\{\mathbf{n}(i)\mathbf{n}^H(i)\} = \sigma^2\mathbf{I}$.

3. TURBO MIMO EQUALIZERS

The receiver first associates the signals from transmit antennas of the kth user to the N_T/n_0 sets of size n_0, so that antennas indexed by $n = 1, \ldots, n_0$ belong to the first set, those indexed by $n = n_0 + 1, \ldots, 2n_0$ belong to the second set and so forth. Thereby the number of transmit antennas N_T is assumed to be an integer multiple of n_0. However, the receiver derivation for the more general cases of users having different numbers of transmit antennas and/or different sets of transmit antennas having different sizes is straightforward. Without loss of generality, the receiver derivation is presented for the first set of transmit antennas of the kth user in Section 3.1. The derivation is exactly the same for the rest of transmit antenna groups and the rest of users, with a difference only in indexing. The SISO channel decoding part and the extrinsic probabilities calculation are presented in Section 3.2. The special cases of $n_0 = 1$ and $n_0 = N_T$ are considered in more detail in Section 3.3. For $n_0 = 1$, only one antenna is detected at a time and the receiver can be viewed as an extension of the receiver presented in [20] to the frequency-selective channel. For $n_0 = N_T$, all the transmit antennas are detected jointly, resulting in the preserved DoFs of the receiver.

3.1. SC/MMSE equalizer derivation

Figure 3 shows the receiver block diagram. First, an estimate $\hat{\mathbf{H}}$ of the channel matrix $\mathbf{H}$ is obtained based on the training sequence $\mathbf{u}(i)$, $i = 1, \ldots, T$. Then, the covariance matrix $\mathbf{R}$ of the UCCI-plus-noise is estimated. In the first iteration, only the training sequence is used for this purpose, resulting in

$$\hat{\mathbf{R}} = \frac{1}{T}\sum_{i=1}^{T}\left(\mathbf{y}(i) - \hat{\mathbf{H}}\mathbf{u}(i)\right)\left(\mathbf{y}(i) - \hat{\mathbf{H}}\mathbf{u}(i)\right)^H. \tag{9}$$

Starting from the second iteration, we make use of the soft feedback from the SISO decoding when estimating the covariance matrix. We denote the soft feedback vector as $\overline{\mathbf{u}}(i)$. Its elements are obtained by replacing the corresponding elements of $\mathbf{u}(i)$ by their soft estimates, defined as

$$\overline{b}_k^{(n)}(i) = \sum_{q=1}^{2^{k_0}} \alpha_q P_{\mathrm{SISO}}^{\mathrm{APP}}\left(b_k^{(n)}(i) = \alpha_q\right), \tag{10}$$

where $P_{\mathrm{SISO}}^{\mathrm{APP}}$ denotes *a posteriori* information obtained after SISO decoding (to be defined in (27)). The covariance matrix estimate is now obtained by

$$\begin{aligned}\hat{\mathbf{R}} = \frac{1}{T}\sum_{i=1}^{T}\left(\mathbf{y}(i) - \hat{\mathbf{H}}\mathbf{u}(i)\right)\left(\mathbf{y}(i) - \hat{\mathbf{H}}\mathbf{u}(i)\right)^H \\ + \frac{1}{B}\sum_{i=T+1}^{T+B}\left(\mathbf{y}(i) - \hat{\mathbf{H}}\overline{\mathbf{u}}(i)\right)\left(\mathbf{y}(i) - \hat{\mathbf{H}}\overline{\mathbf{u}}(i)\right)^H.\end{aligned} \tag{11}$$

The estimate $\hat{\mathbf{R}}$ is, therefore, dependent on the iteration index. However, for the simplicity of notation we omit this dependence, since the receiver derivation is identical for all iterations. Moreover, only in the first iteration (9) is used for the estimation of $\mathbf{R}$, while in all subsequent iterations (11) is used. Let the kth user be the user of interest. We further denote

$$\mathbf{u}_k^{\langle 1\rangle}(i) = \tilde{\mathbf{u}}(i) - \tilde{\mathbf{u}}(i) \odot \mathbf{e}_k^{\langle 1\rangle}, \tag{12}$$

where

$$\mathbf{e}_k^{\langle \gamma\rangle} = [\underbrace{0,\ldots,0}_{[(L-1)K+k-1]N_T+(\gamma-1)n_0}, \underbrace{1,\ldots,1}_{n_0}, \underbrace{0,\ldots,0}_{(LK-k+1)N_T-\gamma n_0}]^{\mathrm{T}}, \tag{13}$$

and $\odot$ and $\gamma = 1,\ldots,N_T/n_0$ denote elementwise vector product and antenna set index, respectively. The vectors $\tilde{\mathbf{u}}(i)$ are obtained by replacing the elements of $\mathbf{u}(i)$ by their soft estimates, that is, an element is

$$\tilde{b}_k^{(n)}(i) = \sum_{q=1}^{2^{k_0}} \alpha_q P_{\mathrm{SISO}}^{\mathrm{ext}}\left(b_k^{(n)}(i) = \alpha_q\right), \tag{14}$$

where $P_{\mathrm{SISO}}^{\mathrm{ext}}$ denotes the extrinsic information obtained after SISO decoding (to be defined in (28)). The signals $b_k^{(n)}(i)$, $n = 1,\ldots,n_0$, are jointly detected by filtering the signal

$$\mathbf{y}_k^{\langle 1\rangle}(i) = \mathbf{y}(i) - \hat{\mathbf{H}}\mathbf{u}_k^{\langle 1\rangle}(i), \quad i = T+1,\ldots,B+T, \tag{15}$$

using a linear MMSE filter whose weighting matrix $\mathbf{W}_k^{\langle 1\rangle}(i)$ satisfies the following criterion:

$$[\mathbf{W}_k^{\langle 1\rangle}(i), \mathbf{A}_k^{\langle 1\rangle}(i)] = \arg\min_{\mathbf{W},\mathbf{A}} ||\mathbf{W}^H\mathbf{y}_k^{\langle 1\rangle}(i) - \mathbf{A}^H\boldsymbol{\beta}_k^{\langle 1\rangle}(i)||^2, \tag{16}$$

subject to the constraint $[\mathbf{A}]_{j,j} = 1$, $j = 1,\ldots,n_0$, to avoid the trivial solution $[\mathbf{W}_k^{\langle 1\rangle}(i), \mathbf{A}_k^{\langle 1\rangle}(i)] = [\mathbf{0},\mathbf{0}]$. $\boldsymbol{\beta}_k^{\langle 1\rangle}(i) \in \mathbb{C}^{n_0\times 1}$ is defined by

$$\boldsymbol{\beta}_k^{\langle 1\rangle}(i) = \left[b_k^{(1)}(i),\ldots,b_k^{(n_0)}(i)\right]^{\mathrm{T}}. \tag{17}$$

It is shown in the Appendix that the matrix $\mathbf{W}_k^{\langle 1\rangle}(i) \in \mathbb{C}^{LN_R\times n_0}$ can be derived as

$$\mathbf{W}_k^{\langle 1\rangle}(i) = \left[\frac{\mathbf{M}_k^{\langle 1\rangle}(i)^{-1}\mathbf{h}_k^{(1)}}{1+\mathbf{h}_k^{(1)H}\mathbf{M}_k^{\langle 1\rangle}(i)^{-1}\mathbf{h}_k^{(1)}} \cdots \frac{\mathbf{M}_k^{\langle 1\rangle}(i)^{-1}\mathbf{h}_k^{(n_0)}}{1+\mathbf{h}_k^{(n_0)H}\mathbf{M}_k^{\langle 1\rangle}(i)^{-1}\mathbf{h}_k^{(n_0)}}\right], \tag{18}$$

where

$$\mathbf{M}_k^{\langle 1\rangle}(i) = \underbrace{\hat{\mathbf{H}}\boldsymbol{\Lambda}_k^{\langle 1\rangle}(i)\hat{\mathbf{H}}^H + \hat{\mathbf{R}}}_{\mathbf{R}_{\mathrm{cov}}^{\langle 1\rangle}} - \sum_{n=1}^{n_0}\mathbf{h}_k^{(n)}\mathbf{h}_k^{(n)H}, \tag{19}$$

and $\mathbf{h}_k^{(n)}$ is the $[(L-1)KN_T+kN_T+n]$th column of the matrix $\hat{\mathbf{H}}$. The matrix $\boldsymbol{\Lambda}_k^{\langle 1\rangle}(i)$ is defined as

$$\begin{aligned}\boldsymbol{\Lambda}_k^{\langle 1\rangle}(i) &= \mathbf{I} - \mathrm{E}\left\{\mathbf{u}_k^{\langle 1\rangle}(i)\mathbf{u}_k^{\langle 1\rangle}(i)^H\right\} \\ &= \mathrm{diag}\Big\{1 - \left|\left[\tilde{\mathbf{u}}(i)\right]_1\right|^2, \ldots, 1 - \left|\left[\tilde{\mathbf{u}}(i)\right]_{(L-1)KN_T}\right|^2, \\ &\qquad \underbrace{1,\ldots,1}_{n_0}, 1 - \left|\left[\tilde{\mathbf{u}}(i)\right]_{(L-1)KN_T+n_0+1}\right|^2, \ldots, \\ &\qquad 1 - \left|\left[\tilde{\mathbf{u}}(i)\right]_{(2L-1)KN_T}\right|^2\Big\}.\end{aligned} \tag{20}$$

Note that (20) holds only for the M-PSK case, although it is straightforward to extend the receiver derivation to the more general signal constellations. Detailed derivation of the optimal solution for a pair of matrices $[\mathbf{W}_k^{\langle 1\rangle}(i), \mathbf{A}_k^{\langle 1\rangle}(i)]$ is given in the Appendix. Assuming that the MMSE filter output $\mathbf{z}_k^{\langle 1\rangle}(i) \in \mathbb{C}^{n_0\times 1}$ can be viewed as the output of the equivalent Gaussian channel [27], we can write

$$\begin{aligned}\mathbf{z}_k^{\langle 1\rangle}(i) &= \mathbf{W}_k^{\langle 1\rangle H}(i)\mathbf{y}_k^{\langle 1\rangle}(i) \\ &= \boldsymbol{\Omega}_k^{\langle 1\rangle}(i)\boldsymbol{\beta}_k^{\langle 1\rangle}(i) + \boldsymbol{\Psi}_k^{\langle 1\rangle}(i),\end{aligned} \tag{21}$$

where matrix $\boldsymbol{\Omega}_k^{\langle 1\rangle}(i) \in \mathbb{C}^{n_0\times n_0}$ contains the gains of the equivalent channel, defined as

$$\boldsymbol{\Omega}_k^{\langle 1\rangle}(i) = \mathrm{E}\left\{\mathbf{z}_k^{\langle 1\rangle}(i)\boldsymbol{\beta}_k^{\langle 1\rangle H}(i)\right\} = \mathbf{W}_k^{\langle 1\rangle H}(i)\boldsymbol{\Pi}_k^{\langle 1\rangle} \tag{22}$$

with $\boldsymbol{\Pi}_k^{\langle 1\rangle}(i) = [\mathbf{h}_k^{(1)}\cdots\mathbf{h}_k^{(n_0)}]$. The vector $\boldsymbol{\Psi}_k^{\langle 1\rangle}(i) \in \mathbb{C}^{n_0\times 1}$ is the equivalent additive Gaussian noise with covariance matrix,

$$\begin{aligned}\boldsymbol{\Theta}_k^{\langle 1\rangle}(i) &= \mathrm{E}\left\{\boldsymbol{\Psi}_k^{\langle 1\rangle}(i)\boldsymbol{\Psi}_k^{\langle 1\rangle H}(i)\right\} \\ &= \mathbf{W}_k^{\langle 1\rangle H}(i)\mathbf{R}_{\mathrm{cov}}^{\langle 1\rangle}\mathbf{W}_k^{\langle 1\rangle}(i) - \boldsymbol{\Omega}_k^{\langle 1\rangle}(i)\boldsymbol{\Omega}_k^{\langle 1\rangle H}(i).\end{aligned} \tag{23}$$

The outputs of the equivalent channels $\mathbf{z}_k^{\langle\gamma\rangle}(i)$ and their parameters $\mathbf{\Omega}_k^{\langle\gamma\rangle}(i)$ and $\mathbf{\Theta}_k^{\langle\gamma\rangle}(i)$ for $\gamma = 1,\ldots,N_T/n_0$ are passed to the APP block that calculates the *extrinsic* probabilities needed for SISO decoding, as described in Section 3.2.

3.2. APP block and SISO decoding

The SISO channel decoding algorithm used in this paper is a symbol-level MAP algorithm from [28]. For the sake of simplicity, we omit the full derivation of the MAP algorithm and we refer to [20, 28]. It should be noted that the input required by the decoder is the probability $P(S_i, S_{i+1})$ associated with the transition between two trellis states, S_i and S_{i+1}, of the STTrC code. The transition probability can be calculated as

$$P(S_i, S_{i+1}) = \prod_{n=1}^{N_T} P_{\mathrm{MMSE}}^{\mathrm{ext}}\left(b_k^{(n)}(i) = d_n^{i,i+1}\right), \tag{24}$$

where $d_n^{i,i+1} \in \mathbb{Q}$ are the encoder outputs that are associated with the transition (S_i, S_{i+1}). $P_{\mathrm{MMSE}}^{\mathrm{ext}}(b_k^{(n)}(i) = \alpha_q)$ are extrinsic probabilities obtained by the MMSE detection. For the first set of jointly detected signals $(n = 1,\ldots,n_0)$, the extrinsic probabilities are calculated in the APP block as

$$P_{\mathrm{MMSE}}^{\mathrm{ext}}\left(b_k^{(n)}(i) = \alpha_q\right) = \sum_{\mathbf{f}\in\mathbf{B}^{d_n}} P\left(\mathbf{z}_k^{\langle 1\rangle}(i)|\mathbf{f}\right)\left[\prod_{p=1,p\neq n}^{n_0} P_{\mathrm{SISO}}^{\mathrm{ext}}\left(b_k^{(n)}(i) = d_n\right)\right], \tag{25}$$

for $q = 1,\ldots,2^{k_0}$ and $n = 1,\ldots,n_0$, where $\mathbf{B}^{d_n} = \{\mathbf{f} \in \mathcal{Q}^{n_0\times 1} \mid f_n = d_n\}$ and

$$P\left(\mathbf{z}_k^{\langle 1\rangle}(i)|\mathbf{f}\right) = e^{-\left(\mathbf{z}_k^{\langle 1\rangle}(i)-\mathbf{\Omega}_k^{\langle 1\rangle}(i)\mathbf{f}\right)^H \mathbf{\Theta}_k^{\langle 1\rangle^{-1}}(i)\left(\mathbf{z}_k^{\langle 1\rangle}(i)-\mathbf{\Omega}_k^{\langle 1\rangle}(i)\mathbf{f}\right)}. \tag{26}$$

Based on the transition probabilities $P(S_i, S_{i+1})$, the SISO channel decoder calculates the *a posteriori* probabilities for the symbols $b_k^{(n)}(i)$, defined as

$$P_{\mathrm{SISO}}^{\mathrm{APP}}\left(b_k^{(n)}(i) = \alpha_q\right) = P\left(b_k^{(n)}(i) = \alpha_q \mid \mathbf{z}_k^{\langle 1\rangle}(i), \mathbf{\Omega}_k^{\langle 1\rangle}(i), \mathbf{\Theta}_k^{\langle 1\rangle}(i),\ i = T+1,\ldots,T+B\right). \tag{27}$$

The decoder extrinsic probability is then calculated as

$$P_{\mathrm{SISO}}^{\mathrm{ext}}\left(b_k^{(n)}(i) = \alpha_q\right) = \frac{P_{\mathrm{SISO}}^{\mathrm{APP}}\left(b_k^{(n)}(i) = \alpha_q\right)}{\left[P_{\mathrm{MMSE}}^{\mathrm{ext}}\left(b_k^{(n)}(i) = \alpha_q\right)\right]^{Q_{\mathrm{ext}}}}. \tag{28}$$

The similar procedure is repeated for all N_T/n_0 groups of transmit antennas that are jointly detected, in order to obtain all probabilities $P_{\mathrm{SISO}}^{\mathrm{ext}}(b_k^{(n)}(i) = \alpha_q)$ for $n = 1,\ldots,N_T$. The parameter Q_{ext} is an ad-hoc parameter that was introduced in [9, 20]. It is shown in [20] that if the value of Q_{ext} is appropriately chosen so as to be between 0 and 1, the receiver performance can be significantly improved. This is due to the fact that the extrinsic information in the initial iterations is not accurate enough, especially with relatively small SNR values. By imposing the parameter Q_{ext}, the effect of this inaccuracy is reduced, at the expense of slower receiver convergence. The result of simulations conducted to evaluate the influence of this parameter on the receiver performance is presented in Section 5.

The receiver complexity is dominated by the MMSE part which requires inversion of the matrix $\mathbf{M}_k^{\langle\gamma\rangle}(i)$ as well as by the APP block which calculates the extrinsic information of the MMSE detector. The overall complexity is therefore $O\{\max(L^3N_R^3, 2^{k_0n_0})\}$. It can be seen that the complexity of the MMSE part does not depend on the number of antennas to be jointly detected. The complexity of the APP part of the receiver, however, increases exponentially with n_0.

3.3. Special cases of $n_0 = 1$ and $n_0 = N_T$

(i) *Receiver* 1, $n_0 = 1$, *transmit antennas detected one-by-one*. Since the complexity of the receiver depends exponentially on n_0, this option has the lowest complexity. Signal from only one antenna is detected at a time, while the rest of the antennas are cancelled by the soft feedback and the MMSE filtering, together with CCI and ISI. By doing this, *effective* DoFs of the receiver are preserved. It should be noted that the number of *effective* DoFs depends on the reliability of the soft feedback information, which can be seen from (19). In the ideal case of perfect feedback (which is not realistic in practice), the number of *effective* DoFs reaches its maximum value, which is equal to $LN_R - 1$. The fact that feedback is nonperfect in reality will result in a number of *effective* DoFs that is smaller than $LN_R - 1$, since the matrix $\mathbf{H}\mathbf{\Lambda}_k^{\langle\gamma\rangle}(i)\mathbf{H}^H - \mathbf{h}_k^{(1)}\mathbf{h}_k^{(1)^H}$ is in general a nonzero matrix. The preserved DoFs are then used to suppress UCCI, if it is present. If the number of *effective* DoFs is large enough so that in the asymptotic case of large SNR the matrix $\mathbf{M}_k^{\langle\gamma\rangle}(i)$ does not have a full rank, then the ISI, CCI, and UCCI can be *perfectly* suppressed. Otherwise, the receivers' performance saturates to an error floor for large SNR values.

(ii) *Receiver* 2, $n_0 = N_T$, *all transmit antennas detected jointly*. In this case, the complexity of the receiver is the largest. However, the $N_T - 1$ *effective* DoFs of the receiver are now *perfectly* preserved. This can be seen from (19). The signals from N_T antennas can be seen as being passed jointly to the receiver output by the third term on the right-hand side of (19). The jointly detected signals are then optimally separated in the APP block. In general, when n_0 out of N_T antennas are detected jointly, the $n_0 - 1$ DoFs are *perfectly* preserved, while *at most* $N_T - n_0$ ones are preserved by soft cancellation, depending on the feedback reliability. Also, one should notice that in the theoretical case of the perfect feedback, the proposed receivers' performance will be identical for any n_0 value.

4. PERFECT FEEDBACK

A lower bound on the receiver performance curve can be obtained in the case of the perfect feedback where all antennas of the single-user signal are detected jointly $(n_0 = N_T)$ using ML detector followed by the MAP-SISO decoder. With the

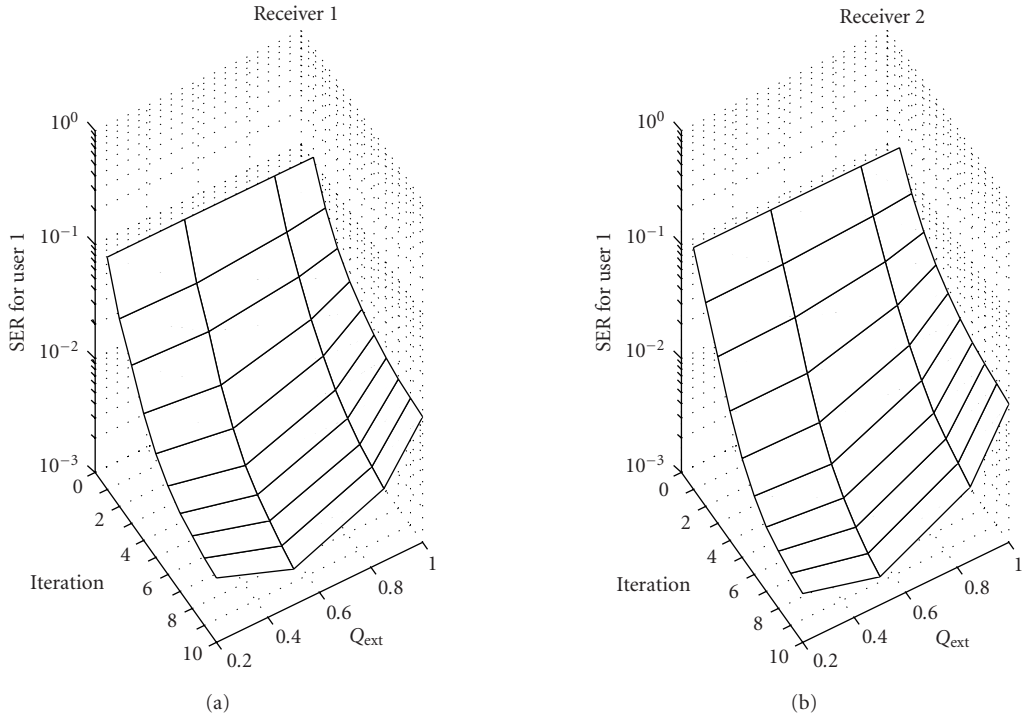

FIGURE 4: Dependence of the receivers' performances on the parameter Q_{ext}, $(K, K_I, N_R) = (1, 0, 1)$, $(B, T) = (150, 15)$, $E_b/N_0 = 9$ dB, $N_T = 2$, $\tau = 0$: (a) receiver 1 and (b) receiver 2.

perfect feedback (15) becomes

$$\mathbf{y}_k^{\langle 1\rangle}(i) = \mathbf{\Pi}_k^{\langle 1\rangle^H} \boldsymbol{\beta}_k^{\langle 1\rangle}(i) + \mathbf{H}_I \mathbf{u}_I(i) + \mathbf{n}(i). \tag{29}$$

The probability associated with the transition (S_i, S_{i+1}) between two trellis states S_i and S_{i+1} can be calculated as

$$P(S_i, S_{i+1}) = e^{-(\mathbf{y}_k^{\langle 1\rangle}(i) - \mathbf{\Pi}_k^{\langle 1\rangle^H} \boldsymbol{\beta}_k^{\langle 1\rangle}(i))^H \hat{\mathbf{R}}^{-1} (\hat{\mathbf{y}}_k^{\langle 1\rangle}(i) - \mathbf{\Pi}_k^{\langle 1\rangle^H} \boldsymbol{\beta}_k^{\langle 1\rangle}(i))}. \tag{30}$$

The receiver described in this section with the assumption of perfect feedback is used in Section 5 to compare with the proposed receivers' performance curves with its lower bound.

5. NUMERICAL EXAMPLES

Performance of the proposed receivers was evaluated through computer simulations. The channel estimates were assumed to be perfect. All users transmitted with the same power, and fading was constant over each transmitted frame, but changed independently frame-by-frame. The fading was assumed to be frequency selective with the number of paths $L = 5$, each of which is Rayleigh distributed and uncorrelated. It was assumed that antennas are spatially uncorrelated, and that signals at all receive antennas have the same average powers. E_s/N_0 is defined as the SNR per symbol per receive antenna. The exponentially decaying power delay profile with decay exponent $-\tau$ was assumed, so that $\tau = 0$ results in the equal-average-power-multipath and $\tau \to \infty$ in the flat-fading channels, respectively. The 4-state QPSK code with $N_T = 2$ presented in [4] was used to encode signals of all MIMO users. All the users transmit with the same powers. The log-MAP space-time trellis decoder shown in [20, 28] was used. User-specific random interleavers were assumed.

As mentioned in Section 3.1 it is shown in [20] that the appropriate choice of parameter Q_{ext} significantly improves the receiver performance in a flat-fading case for $n_0 = 1$. The same approach was used in the simulations and the impact of the parameter Q_{ext} in the multipath channel with $\tau = 0$ for the receivers (receiver 1 and receiver 2) was first evaluated. The results are presented in Figure 4 for the case of $(K, K_I, N_R) = (1, 0, 1)$. The symbol error rate (SER) versus iteration index and Q_{ext} is presented. It can be seen that $Q_{\text{ext}} = 0.5$ yields the best performance for both receivers. Therefore, this value was used in the further simulations.

In Figure 5, SER and frame error rate (FER) performances of receivers 1 and 2 are presented versus per-antenna E_s/N_0 for $(K, K_I, N_R) = (1, 0, 1)$ and $\tau = 0$ with the iteration number as a parameter. It is seen that receiver 2 offers performance improvement over receiver 1, due to the joint detection of all transmit antennas. The gain, however, is not very large. This is due to the fact that the effective number of DoFs is increased only by the factor of 1 with the joint detection. Also the feedback is relatively reliable and the DoFs can be preserved almost equally well with soft cancellation as with the joint detection. The performance of the receiver with perfect-feedback and ML detection is also shown for comparison.

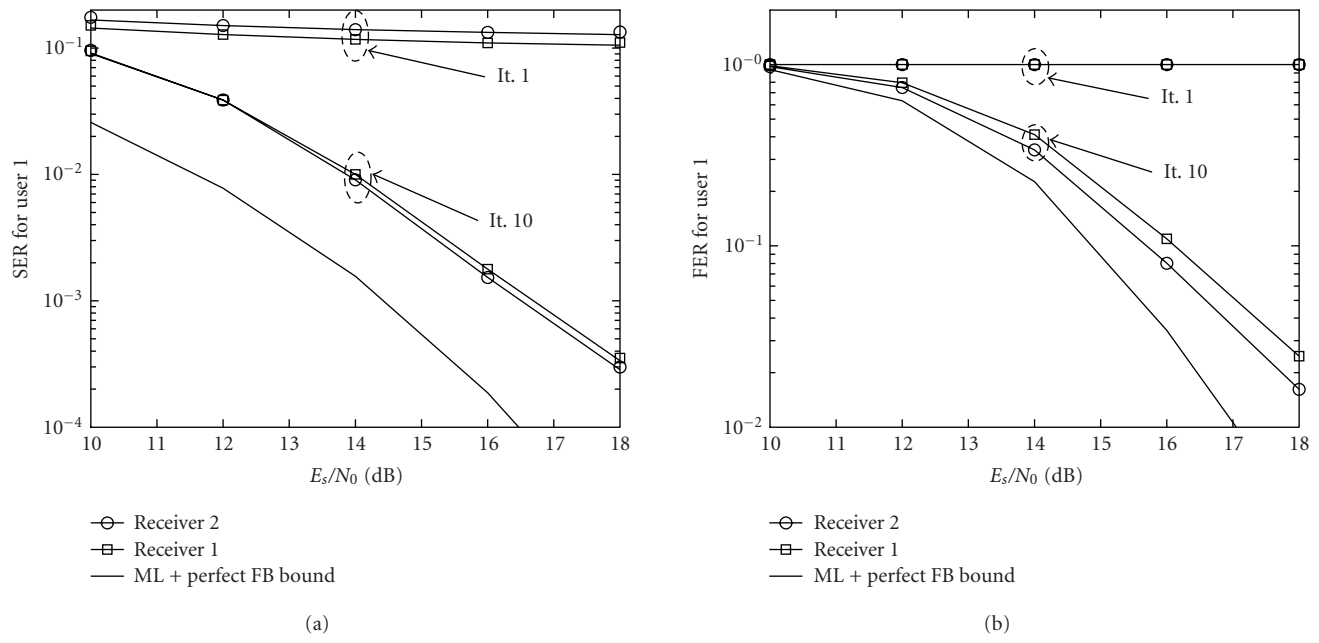

FIGURE 5: Receivers 1's and 2's performance versus per-antenna E_s/N_0; $(K, K_I, N_R) = (1, 0, 1)$, $(B, T) = (150, 15)$, $N_T = 2$, $\tau = 0$. (a) Symbol error rate and (b) frame error rate. FB = feedback. It. = iteration index.

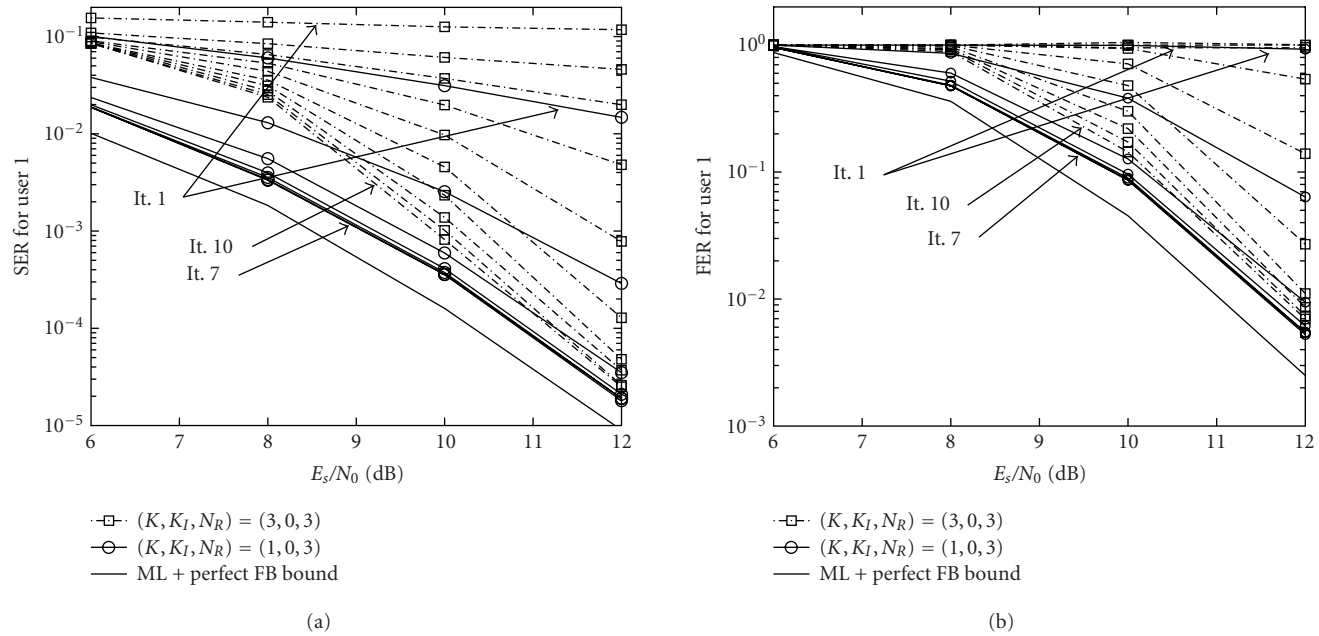

FIGURE 6: Receiver 1's performance versus per-antenna E_s/N_0; $(K, K_I, N_R) = (3, 0, 3)$, $(B, T) = (150, 15)$, $N_T = 2$, $\tau = 0$. (a) Symbol error rate and (b) frame error rate. FB = feedback. It. = iteration index.

In Figure 6, the SER and FER performances of receiver 1 are presented versus per-antenna E_s/N_0, for $(K, K_I, N_R) = (3, 0, 3)$ and $\tau = 0$ with the iteration number as a parameter. In Figure 7, the same set of curves is given for the receiver 2. It is seen that the single-user bound can be achieved after approximately 8 iterations. It should be noticed that with $(K, K_I, N_R) = (1, 0, 3)$, the performances of both receivers after 5 iterations are within only 0.5 dB from the perfect-feedback bound. It is important to mention that the number of receive antennas required to achieve the single-user bound is equal to the number of *users* and not to the *total number of transmit antennas*, as it was the case in [20] for the flat fading. It can also be seen from Figures 6 and 7 that receiver 2 slightly outperforms receiver 1. The reason for the relatively small gains is very similar to that given for the situation described in Figure 5.

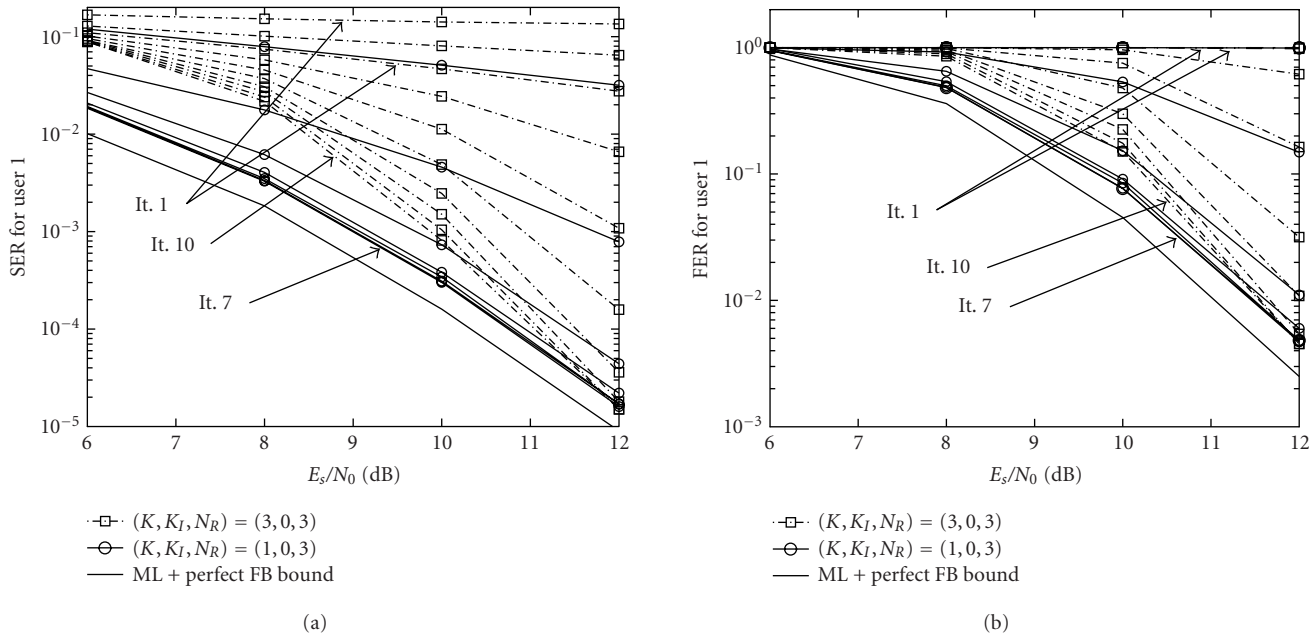

FIGURE 7: Receiver 2's performance versus per-antenna E_s/N_0; $(K, K_I, N_R) = (3, 0, 3)$, $(B, T) = (150, 15)$, $N_T = 2$, $\tau = 0$. (a) Symbol error rate and (b) frame error rate. FB = feedback. It. = iteration index.

Figure 8 shows SER and FER performances of both receivers versus per-antenna E_s/N_0 for $(K, K_I, N_R) = (2, 1, 3)$. It was assumed in this scenario that the UCCI uses only a single antenna. The simulation results for two values of signal-to-UCCI-interference ratio (SIR) are presented. In the cases of SIR equal to 3 dB and 0 dB, the power of the signal transmitted from the UCCI's antenna was assumed to be the same as the power of the signal from the single and two antennas of any of the desired users, respectively. For comparison, the single-user bound described by $(K, K_I, N_R) = (1, 0, 3)$ is presented. It can be seen that both receivers are rather robust against the presence of unknown interference in a wide range of E_s/N_0 values, for both SIR values. Moreover, in case of SIR $= 3$ dB, the receivers can *perfectly* suppress the UCCI if the E_s/N_0 value becomes large. This is due to the fact that after convergence the receivers have enough *effective* DoFs to separate and detect two desired users' signals and suppress one UCCI. It can also be seen from Figure 8 that receivers 1 and 2 show very similar performance. This is due to the fact that the soft feedback is relatively reliable and preserving one additional DoF is of less significance.

In Figure 9, SER and FER performances of both receivers are presented versus per-antenna E_s/N_0 for $(K, K_I, N_R) = (2, 1, 3)$. In this scenario, the UCCI uses two antennas in the same way as the desired users. The curves are plotted with SIR, frame length B, and channel decay exponent τ as parameters. For comparison, the single-user bound described by $(K, K_I, N_R) = (1, 0, 3)$ is also presented. It can be seen again that both receivers are robust against interference over a wide range of E_s/N_0 values. However, due to the lack of *effective* DoFs, the performance curves tend to saturate an error floor with high E_s/N_0 values. This can be solved in a straightforward manner by adding more receive antennas. However, it should be noted from Figure 9 that the error floor can be reduced by increasing the frame length while keeping the ratio T/B constant. This behavior can be explained by two reasons: first, increasing the frame length results in more samples for $\mathbf{R}$ estimation; second, the feedback becomes more accurate with the increased frame length.

It can also be seen by comparing the results for $\tau \to 0$ and $\tau \to \infty$ from Figure 9 that the gain from using receiver 2 is larger if the number of significant multipath components is smaller. This is due to the fact that in the rich multipath environment ($\tau \to 0$), the number of *effective* DoFs is much smaller than the number needed to perfectly suppress the UCCI. Therefore, preserving one DoF with the receiver 2 does not have any significant impact on the receivers' performance. On the other hand, in the flat fading, ($\tau \to \infty$) the number of *effective* DoFs is comparable to the number needed to suppress the UCCI, and preserving one DoF improves performance. The performances of both receivers improve with increased SIR and in the absence of UCCI they are expected to approach the corresponding single-user bounds.

6. CONCLUSIONS

New iterative receiver schemes for the STTrC-coded multiuser system in frequency-selective channels have been derived for single-carrier broadband signalling. It has been shown through computer simulations that the receiver that jointly detects signals from all the transmit antennas of the user of interest performs slightly better than the receiver that

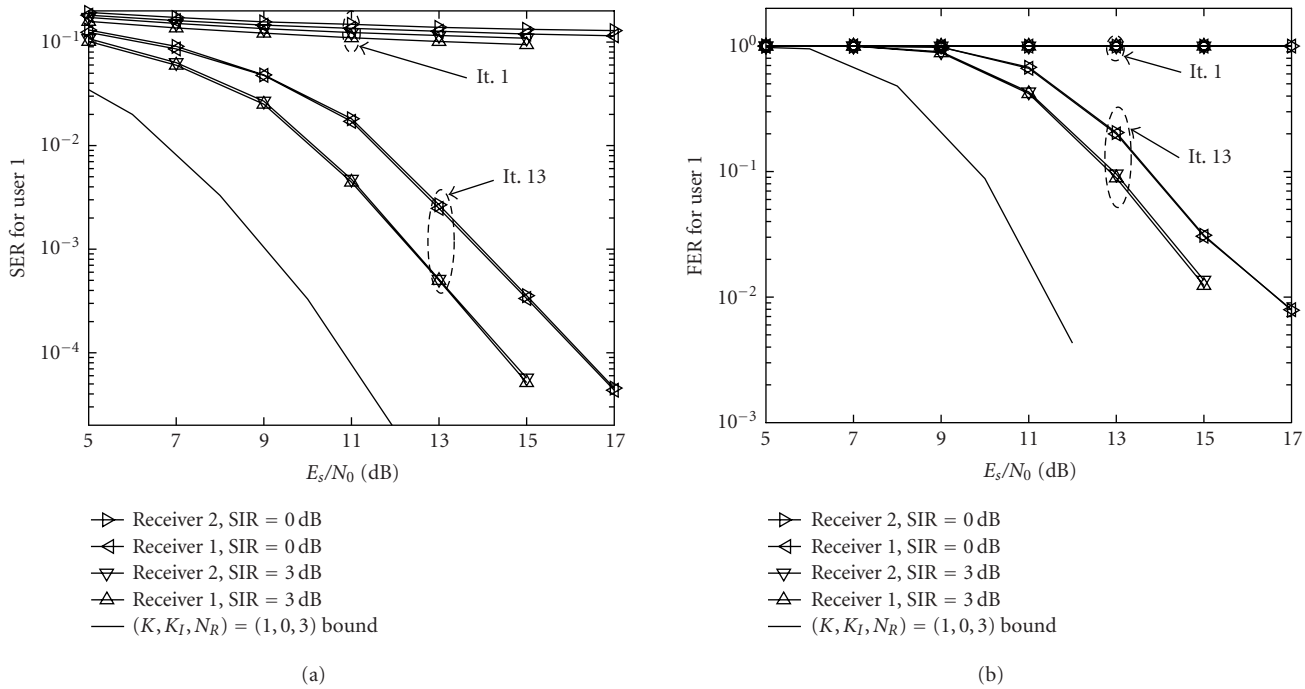

FIGURE 8: Receiver 1's and 2's performance versus per-antenna E_s/N_0; $(K, K_I, N_R) = (2, 1, 3)$, $(B, T) = (150, 15)$, $N_T = 2$, SIR = 0 and 3 dB (single antenna used by UCCI), $\tau = 0$. (a) Symbol error rate and (b) frame error rate.

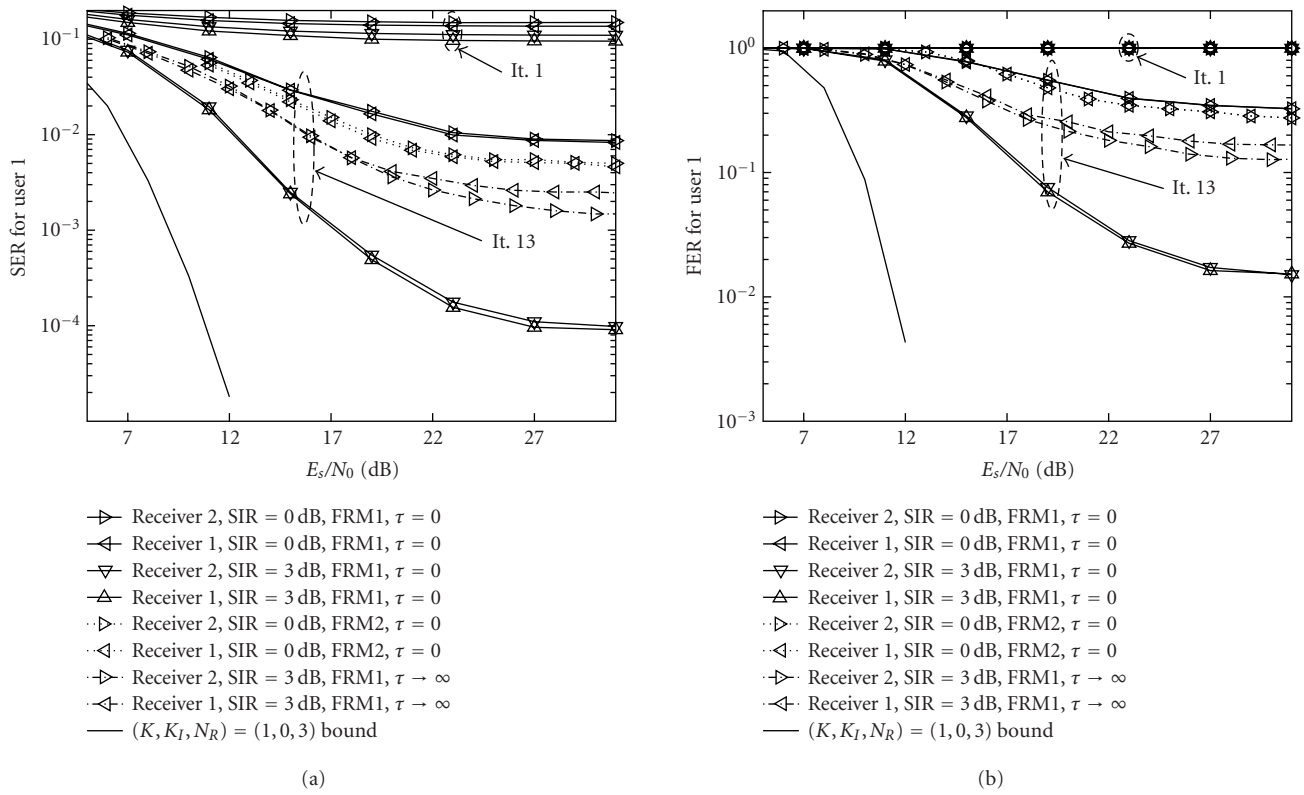

FIGURE 9: Receiver 1's and 2's performance versus per-antenna E_s/N_0, $(K, K_I, N_R) = (2, 1, 3)$, $(B, T) = (150, 15)$ and $(300, 30)$, $N_T = 2$, SIR = 0 and 3 dB (two antennas used by UCCI), $\tau = 0$ and ∞. (a) Symbol error rate and (b) frame error rate. FRM1 : $(B, T) = (150, 15)$. FRM2 : $(B, T) = (300, 30)$.

detects only one antenna at a time. In the presence of relatively strong UCCI, the gain from joint detection is larger if the channel has less multipath components. This is due to the fact that preserving DoFs of the receivers with the joint detection has a greater impact on performance if the number of effective DoFs is comparable to the number needed to perfectly suppress UCCI. The complexity of the MMSE part of the receiver is independent of the number of antennas n_0 that are to be jointly detected. However, the complexity of the APP part, that calculates the extrinsic probabilities needed for SISO channel decoding, grows exponentially with n_0. It has been shown that the performance of both receivers improves by increasing frame length, due to the improved feedback reliability. The performance also improves with higher SIR values. The gain from joint detection, however, is smaller if the feedback is more reliable.

In a multiuser scenario without UCCI, the proposed receivers can achieve corresponding single-user bounds. Thereby, the required number of receive antennas is equal to the number of users and not to the total number of transmit antennas. Furthermore, the receivers' single-user performances are very similar to each other and relatively close to the performance of the ML receiver with perfect feedback.

Future work may include further receiver structure generalization, where the antennas from more than one user are to be detected jointly. This would result in more DoFs that can be used for the UCCI cancellation. It is also of interest to determine the maximum number of users K for which the single-user bound can be achieved with $N_R = K$ receive antennas with N_T as a parameter. Further study is also required to evaluate the receivers' sensitivity to the spatial correlation. The joint detection is expected to be more robust than the antenna-by-antenna detection [29].

APPENDIX

Without loss of generality, derivation of the optimal pair $[\mathbf{W}_k^{\langle 1\rangle}(i), \mathbf{A}_k^{\langle 1\rangle}(i)]$ of matrices is presented only for the first group of n_0 jointly detected antennas. The derivation is similar for the other groups, with difference only in indexing. We denote the nth columns of the matrices $\mathbf{W}_k^{\langle 1\rangle}(i)$ and $\mathbf{A}_k^{\langle 1\rangle}(i)$ as $\mathbf{w}^{(n)}$ and $\mathbf{a}^{(n)}$, respectively. For simplicity of notation, we omit the dependence of $\mathbf{w}^{(n)}$ and $\mathbf{a}^{(n)}$ on user index k, antenna group index γ, and time instant i. The cost function in (16) that is to be minimized can be written as

$$\mathcal{J}\left(\mathbf{W}_k^{\langle 1\rangle}(i), \mathbf{A}_k^{\langle 1\rangle}(i)\right) = \mathrm{E}\left\{\sum_{n=1}^{n_0} \left|\mathbf{m}^{(n)H}\mathbf{g}\right|^2\right\}, \tag{A.1}$$

where

$$\mathbf{m}^{(n)} = \left[\mathbf{w}^{(n)H}, -\mathbf{a}^{(n)H}\right]^H \tag{A.2}$$

with

$$\mathbf{g} = \left[\mathbf{y}_k^{\langle 1\rangle}(i)^H, \boldsymbol{\beta}_k^{\langle 1\rangle}(i)^H\right]^H. \tag{A.3}$$

This is equivalent to minimizing each of the component cost functions, defined as

$$\mathcal{J}^{(n)}\left(\mathbf{m}^{(n)}\right) = \mathrm{E}\left\{\left|\mathbf{m}^{(n)H}\mathbf{g}\right|^2\right\}. \tag{A.4}$$

To avoid the trivial solution, $[\mathbf{a}^{(n)}]_n$ is set to be equal to 1. Introducing the Lagrange multiplier λ, the equivalent cost function to be minimized becomes

$$\mathcal{J}_{\mathrm{eq}}^{(n)}\left(\mathbf{m}^{(n)}\right) = \mathrm{E}\left\{\left|\mathbf{m}^{(n)H}\mathbf{g}\right|^2\right\} - \lambda\left(\mathbf{m}^{(n)H}\mathbf{j}^{(n)} = 1\right), \tag{A.5}$$

where

$$\mathbf{j}^{(n)} = \left[\mathbf{0}_{1\times(n-1)} \quad 1 \quad \mathbf{0}_{1\times(n_0-n)}\right]^{\mathrm{T}}. \tag{A.6}$$

Differentiating (A.5) with respect to $\mathbf{m}^{(n)}$ gives

$$\frac{\partial \mathcal{J}_{\mathrm{eq}}^{(n)}\left(\mathbf{m}^{(n)}\right)}{\partial \mathbf{m}^{(n)}} = \mathbf{R}_{\mathbf{gg}}\mathbf{m}^{(n)} - \lambda\mathbf{j}^{(n)}, \tag{A.7}$$

where

$$\mathbf{R}_{\mathbf{gg}} = \begin{bmatrix} \mathbf{R}_{\mathrm{cov}}^{\langle 1\rangle} & \boldsymbol{\Pi}_k^{\langle 1\rangle} \\ \boldsymbol{\Pi}_k^{\langle 1\rangle H} & \mathbf{I}_{n_0\times n_0} \end{bmatrix}. \tag{A.8}$$

From (A.7), the optimal value of $\mathbf{m}^{(n)}$ can be found as

$$\mathbf{m}^{(n)} = \frac{\mathbf{R}_{\mathbf{gg}}^{-1}\mathbf{j}^n}{\mathbf{j}^{(n)H}\mathbf{R}_{\mathbf{gg}}^{-1}\mathbf{j}^{(n)}}. \tag{A.9}$$

Applying the property of the inverse of the block-matrix [30]

$$\begin{bmatrix} \mathbf{A} & \mathbf{B} \\ \mathbf{C} & \mathbf{D} \end{bmatrix}^{-1} = \begin{bmatrix} \mathbf{Q}^{-1} & -\mathbf{Q}^{-1}\mathbf{B}\mathbf{D}^{-1} \\ -\mathbf{D}^{-1}\mathbf{C}\mathbf{Q}^{-1} & \mathbf{D}^{-1}\left(\mathbf{I}+\mathbf{C}\mathbf{Q}^{-1}\mathbf{B}\mathbf{D}^{-1}\right) \end{bmatrix} \tag{A.10}$$

to the inverse of matrix $\mathbf{R}_{\mathbf{gg}}$, where $\mathbf{Q} = \mathbf{A} - \mathbf{B}\mathbf{D}^{-1}\mathbf{C}$, we obtain

$$\mathbf{m}^{(n)} = \begin{bmatrix} \dfrac{\mathbf{M}_k^{\langle 1\rangle}(i)^{-1}\mathbf{h}_k^{(n)}}{1+\mathbf{h}_k^{(n)H}\mathbf{M}_k^{\langle 1\rangle}(i)^{-1}\mathbf{h}_k^{(n)}} \\ \dfrac{\mathbf{h}_k^{(n)H}\mathbf{M}_k^{\langle 1\rangle}(i)^{-1}\mathbf{h}_k^{(1)}}{1+\mathbf{h}_k^{(n)H}\mathbf{M}_k^{\langle 1\rangle}(i)^{-1}\mathbf{h}_k^{(n)}} \\ \vdots \\ \dfrac{\mathbf{h}_k^{(n)H}\mathbf{M}_k^{\langle 1\rangle}(i)^{-1}\mathbf{h}_k^{(n-1)}}{1+\mathbf{h}_k^{(n)H}\mathbf{M}_k^{\langle 1\rangle}(i)^{-1}\mathbf{h}_k^{(n)}} \\ 1 \\ \dfrac{\mathbf{h}_k^{(n)H}\mathbf{M}_k^{\langle 1\rangle}(i)^{-1}\mathbf{h}_k^{(n+1)}}{1+\mathbf{h}_k^{(n)H}\mathbf{M}_k^{\langle 1\rangle}(i)^{-1}\mathbf{h}_k^{(n)}} \\ \vdots \\ \dfrac{\mathbf{h}_k^{(n)H}\mathbf{M}_k^{\langle 1\rangle}(i)^{-1}\mathbf{h}_k^{(n_0)}}{1+\mathbf{h}_k^{(n)H}\mathbf{M}_k^{\langle 1\rangle}(i)^{-1}\mathbf{h}_k^{(n)}} \end{bmatrix}, \tag{A.11}$$

from which it follows that

$$\mathbf{w}^{(n)} = \frac{\mathbf{M}_k^{\langle 1\rangle}(i)^{-1}\mathbf{h}_k^{(n)}}{1+\mathbf{h}_k^{(n)H}\mathbf{M}_k^{\langle 1\rangle}(i)^{-1}\mathbf{h}_k^{(n)}},$$

$$\mathbf{a}^{(n)} = \begin{bmatrix} \dfrac{\mathbf{h}_k^{(n)H}\mathbf{M}_k^{\langle 1\rangle}(i)^{-1}\mathbf{h}_k^{(1)}}{1+\mathbf{h}_k^{(n)H}\mathbf{M}_k^{\langle 1\rangle}(i)^{-1}\mathbf{h}_k^{(n)}} \\ \vdots \\ \dfrac{\mathbf{h}_k^{(n)H}\mathbf{M}_k^{\langle 1\rangle}(i)^{-1}\mathbf{h}_k^{(n-1)}}{1+\mathbf{h}_k^{(n)H}\mathbf{M}_k^{\langle 1\rangle}(i)^{-1}\mathbf{h}_k^{(n)}} \\ 1 \\ \dfrac{\mathbf{h}_k^{(n)H}\mathbf{M}_k^{\langle 1\rangle}(i)^{-1}\mathbf{h}_k^{(n+1)}}{1+\mathbf{h}_k^{(n)H}\mathbf{M}_k^{\langle 1\rangle}(i)^{-1}\mathbf{h}_k^{(n)}} \\ \vdots \\ \dfrac{\mathbf{h}_k^{(n)H}\mathbf{M}_k^{\langle 1\rangle}(i)^{-1}\mathbf{h}_k^{(n_0)}}{1+\mathbf{h}_k^{(n)H}\mathbf{M}_k^{\langle 1\rangle}(i)^{-1}\mathbf{h}_k^{(n)}} \end{bmatrix}. \tag{A.12}$$

After repeating similar procedure for all the n_0 transmit antennas from the first group of the kth user, the optimal pair of matrices $[\mathbf{W}_k^{\langle 1\rangle}(i), \mathbf{A}_k^{\langle 1\rangle}(i)]$ is obtained as

$$\mathbf{W}_k^{\langle 1\rangle}(i) = [\mathbf{w}^{(1)}, \ldots, \mathbf{w}^{(n_0)}], \qquad \mathbf{A}_k^{\langle 1\rangle}(i) = [\mathbf{a}^{(1)}, \ldots, \mathbf{a}^{(n_0)}]. \tag{A.13}$$

ACKNOWLEDGMENT

The authors gratefully acknowledge Nokia, Elektrobit, Finnish Air Forces, Instrumentointi, National Technology Agency of Finland (Tekes), Nokia Foundation, and Infotech Oulu Graduate School for their support and the anonymous reviewers for their helpful comments.

REFERENCES

[1] E. Telatar, "Capacity of multi-antenna Gaussian channels," *European Transactions on Telecommunications*, vol. 10, no. 6, pp. 585–595, 1999.

[2] G. J. Foschini, "Layered space-time architecture for wireless communication in a fading environment when using multiple antennas," *Bell Labs Technical Journal*, vol. 1, no. 2, pp. 41–59, 1996.

[3] S. M. Alamouti, "A simple transmit diversity technique for wireless communications," *IEEE Journal on Selected Areas in Communications*, vol. 16, no. 8, pp. 1451–1458, 1998.

[4] V. Tarokh, N. Seshadri, and A. R. Calderbank, "Space-time codes for high data rate wireless communication: performance criterion and code construction," *IEEE Transactions on Information Theory*, vol. 44, no. 2, pp. 744–765, 1998.

[5] V. Tarokh, A. Naguib, N. Seshadri, and A. R. Calderbank, "Space-time codes for high data rate wireless communication: performance criteria in the presence of channel estimation errors, mobility, and multiple paths," *IEEE Trans. Communications*, vol. 47, no. 2, pp. 199–207, 1999.

[6] Y. Gong and K. B. Letaief, "Performance evaluation and analysis of space-time coding in unequalized multipath fading links," *IEEE Trans. Communications*, vol. 48, no. 11, pp. 1778–1782, 2000.

[7] L. Hanzo, W. Webb, and T. Keller, *Single and Multicarrier Quadrature Amplitude Modulation*, John Wiley & Sons, New York, NY, USA, 2000.

[8] L. R. Bahl, J. Cocke, F. Jelinek, and J. Raviv, "Optimal decoding of linear codes for minimizing symbol error rate," *IEEE Transactions on Information Theory*, vol. 20, no. 2, pp. 284–287, 1974.

[9] C. Douillard, C. B. M. Jezequel, C. Berrou, A. Picart, P. Didier, and A. Glavieux, "Iterative correction of intersymbol interference: turbo-equalisation," *European Transactions on Telecommunications*, vol. 6, no. 5, pp. 507–511, 1995.

[10] G. Bauch and A. Naguib, "MAP equalization of space-time coded signals over frequency selective channels," in *Proc. IEEE Wireless Communications and Networking Conference (WCNC '99)*, vol. 1, pp. 261–265, New Orleans, La, USA, September 1999.

[11] G. Bauch and N. Al-Dhahir, "Reduced-complexity space-time turbo-equalization for frequency-selective MIMO channels," *IEEE Transactions on Wireless Communications*, vol. 1, no. 4, pp. 819–828, 2002.

[12] B. L. Yeap, C. H. Wong, and L. Hanzo, "Reduced complexity in-phase/quadrature-phase turbo equalisation using iterative channel estimation," in *Proc. IEEE International Conference on Communications (ICC '01)*, vol. 2, pp. 393–397, Helsinki, Finland, June 2001.

[13] L. Hanzo, T. H. Liew, and B. L. Yeap, *Turbo Coding, Turbo Equalisation and Space-Time Coding for Transmission over Fading Channels*, John Wiley & Sons, Chichester, UK, 2002.

[14] D. Reynolds and X. Wang, "Low-complexity turbo-equalization for diversity channels," *Signal Processing*, vol. 81, no. 5, pp. 989–995, 2001.

[15] X. Wang and H. V. Poor, "Iterative (turbo) soft interference cancellation and decoding for coded CDMA," *IEEE Trans. Communications*, vol. 47, no. 7, pp. 1046–1061, 1999.

[16] M. Tüchler, A. C. Singer, and R. Koetter, "Minimum mean squared error equalization using a priori information," *IEEE Trans. Signal Processing*, vol. 50, no. 3, pp. 673–683, 2002.

[17] M. Tüchler, R. Koetter, and A. C. Singer, "Turbo equalization: principles and new results," *IEEE Trans. Communications*, vol. 50, no. 5, pp. 754–767, 2002.

[18] T. Abe and T. Matsumoto, "Space-time turbo equalization in frequency-selective MIMO channels," *IEEE Trans. Vehicular Technology*, vol. 52, no. 3, pp. 469–475, 2003.

[19] H. Omori, T. Asai, and T. Matsumoto, "A matched filter approximation for SC/MMSE iterative equalizers," *IEEE Communications Letters*, vol. 5, no. 7, pp. 310–312, 2001.

[20] B. Lu and X. Wang, "Iterative receivers for multiuser space-time coding systems," *IEEE Journal on Selected Areas in Communications*, vol. 18, no. 11, pp. 2322–2335, 2000.

[21] T. Abe, S. Tomisato, and T. Matsumoto, "A MIMO turbo equalizer for frequency-selective channels with unknown interference," *IEEE Trans. Vehicular Technology*, vol. 52, no. 3, pp. 476–482, 2003.

[22] D. Reynolds and X. Wang, "Turbo multiuser detection with unknown interferers," *IEEE Trans. Communications*, vol. 50, no. 4, pp. 616–622, 2002.

[23] J. Li, K. B. Letaief, and Z. Cao, "Adaptive cochannel interference cancellation in space-time coded communication systems," *IEEE Trans. Communications*, vol. 50, no. 10, pp. 1580–1583, 2002.

[24] C. B. Papadias and H. Huang, "Linear space-time multiuser detection for multipath CDMA channels," *IEEE Journal on Selected Areas in Communications*, vol. 19, no. 2, pp. 254–265, 2001.

[25] A. F. Naguib, N. Seshadri, and A. R. Calderbank, "Applications of space-time block codes and interference suppression for high capacity and high data rate wireless systems," in *Proc. 36th Asilomar Conference on Signals, Systems & Computers*, vol. 2, pp. 1803–1810, Pacific Grove, Calif, USA, November 1998.

[26] A. F. Naguib, V. Tarokh, N. Seshadri, and A. R. Calderbank, "A space-time coding modem for high-data-rate wireless communications," *IEEE Journal on Selected Areas in Communications*, vol. 16, no. 8, pp. 1459–1478, 1998.

[27] H. V. Poor and S. Verdú, "Probability of error in MMSE multiuser detection," *IEEE Transactions on Information Theory*, vol. 43, no. 3, pp. 858–871, 1997.

[28] S. Benedetto, D. Divsalar, G. Montorsi, and F. Pollara, "A soft-input soft-output APP module for iterative decoding of concatenated codes," *IEEE Communications Letters*, vol. 1, no. 1, pp. 22–24, 1997.

[29] N. R. Veselinovic, T. Matsumoto, and C. Scheider, "Reducing performance sensitivity to spatial correlation and timing offset in space-time-coded MIMO turbo equalization," to appear in *IEICE Transactions on Communications*.

[30] G. H. Golub and C. F. Van Loan, *Matrix Computations*, Johns Hopkins University Press, Baltimore, Md, USA, 2nd edition, 1989.

Nenad Veselinovic was born in Valjevo, Serbia and Montenegro, in 1975. He received his M.S., in electrical engineering from the University of Belgrade, Belgrade, Serbia and Montenegro, in 1999. In 2000, he joined the Centre for Wireless Communications, University of Oulu, Oulu, Finland, where he is currently working as a Research Scientist. Mr. Veselinovic is working towards the Ph.D. degree in the field of wireless communications. His main research interests are in statistical signal processing and receiver design for broadband wireless communications. He is a Student Member of the IEEE.

Tad Matsumoto received his B.S., M.S., and Ph.D. degrees in electrical engineering from Keio University, Yokohama-shi, Japan, in 1978, 1980, and 1991, respectively. He joined Nippon Telegraph and Telephone Corporation (NTT) in April 1980. From April 1980 to January 1991, he researched signal transmission techniques, such as modulation/demodulation, error control, and radio link design schemes for 1st- and 2nd-generation mobile communications systems. In July 1992, he transferred to NTT DoCoMo, where he researched code-division multiple-access (CDMA) techniques. From 1992 to 1994, he served as a part-time lecturer at Keio University. In April 1994, he transferred to NTT America, where he served as a Senior Technical Advisor in the NTT-NEXTEL Communications joint project. In March 1996, he returned to NTT DoCoMo, and he was appointed a Head of Radio Signal Processing Laboratory at NTT DoCoMo, where he researched adaptive signal processing, MIMO turbo signal detection, interference cancellation, and space-time coding techniques for broadband mobile communications. In May 2002, he moved to the University of Oulu, Finland, where he is a Professor at the Centre for the Wireless Communications. Presently, he is serving as a Board-of-Governor of the IEEE VT Society for a term from January 2002 to December 2004.

Markku Juntti received his M.S. and Dr.Sc. degrees in electrical engineering from University of Oulu, Oulu, Finland, in 1993 and 1997, respectively. Dr. Juntti has been with University of Oulu since 1992. In 1994–1995, he was a Visiting Research Scientist at Rice University, Houston, Texas. In 1999–2000, he was with Nokia Networks as a Senior Specialist. Dr. Juntti has been a Professor of Telecommunications at University of Oulu since 2000. His research interests include communication and information theory, signal processing for wireless communication systems as well as their application in wireless communication system design. He is an author or coauthor in some 120 papers published in international journals and conference records as well as in book *WCDMA for UMTS* published by Wiley. Dr. Juntti is a Senior Member of IEEE, and an Associate Editor for IEEE Transactions on Vehicular Technology. He was Secretary of IEEE Communication Society Finland Chapter in 1996–1997 and the Chairman for years 2000–2001. He has been a Secretary of the Technical Program Committee of the 2001 IEEE International Conference on Communications (ICC '01), and is the Cochair of the Technical Program Committee of 2004 Nordic Radio Symposium.